eSim 2018
«BUILDING SIMULATION TO SUPPORT BUILDING SUSTAINABILITY»
IBPSA Canada
The Canadian Chapter of the International Building Performance Simulation Association
Le chapitre canadien de International Building Performance Simulation Association

Predicting the Interaction Between Building Integrated Photovoltaics and the Built Environment: Opportunities and Challenges

Ryan Danks[1], Goncalo Pedro[2]

[1] RWDI, Guelph, Ontario Canada
[2] RWDI, Toronto, Ontario, Canada

Abstract: *To achieve ambitious sustainability goals, many building designers are turning to photovoltaic (PV) systems to provide onsite energy production. Increasingly, PV systems are integrated into the building envelope itself. Aside from the non-trivial task of simulating energy generation potential on complex facades in urban environments, understanding the effects of building integrated PV (BIPV) systems on their surrounds also needs to be understood early in the design process to prevent potentially problematic impacts. This paper investigates how modelling inputs influence the accuracy of energy production simulations, to ensure robust predictions which account for the effects of shading and micro-shading of the panels at short time scales in complex urban environments. The potentially problematic secondary effects of BIPV, including visual glare, snow accumulation, and thermal impacts on people and/or ventilation systems are introduced, and approaches to predict and mitigate those impacts are discussed.*

Keywords: *BIPV, photovoltaics, urban analysis, solar simulation*

INTRODUCTION

To achieve ambitious sustainability goals, many building designers are turning to photovoltaic (PV) systems to provide renewable onsite energy production. Increasingly, PV systems are integrated into the building envelope itself, creating façades that are multifunctional. This increased functionality comes at a cost, with panels being oriented less than optimally and being exposed to more complex shading environments.

Traditionally, a simple electricity production estimate is used to calculate viability and payback. This estimate is generally taken from solar maps or, in some cases, calculated using desktop or online tools such as PVWatts produced by the National Renewable Energy Laboratory (NREL) (Dobos, 2014) or RETScreen (NRC 2005). This is generally sufficiently accurate in the case of ground mounted or simple roof mounted systems where there are few or no surrounds and limited potential for energy-reducing shade. In some cases, there is a desire to maximize the amount of PV installed which means encroaching on areas near other equipment and building features or employing PV in non-traditional locations (e.g. façades). In these instances, using simplified calculation methods can result in unacceptable errors.

Aside from the non-trivial task of predicting energy generation potential on complex facades in urban environments, understanding the effects of building integrated PV (BIPV) systems on their surrounds also needs to be understood early in the design process to prevent problematic post-construction impacts including glare, heat gains on people/property and increased structural loads (Chiabrando, 2009).

This paper investigates the appropriateness of traditional modelling approaches and inputs when predicting BIPV energy production through simulation, to ensure accurate predictions which account for the effects of shading and micro-shading of the panels at short time scales and on complex building envelopes. Other potential secondary effects that BIPV systems can have on their surroundings are also discussed including the modelling and simulation process that can be used in each case. These secondary effects include: visual glare, snow accumulation and thermal impacts on people and/or ventilation systems.

SOLAR SIMULATION AND PANEL PERFORMANCE

Solar simulation tools can be used to increase the accuracy of generation estimates. This type of analysis takes building and panel geometry into account along with the shading created by surrounding structures. Although these types of tools can yield more accurate estimates they do require greater input from the user. This increased flexibility increases the potential for user or process error, potentially negating the benefits of using a more detailed analysis. This section focusses on the potential pitfalls and sensitivities that accompany this type of analysis.

Solar Simulation Methodology

The solar simulations were performed using a custom simulation tool developed by the authors (Danks, 2014). Details can be found in the reference, but in general, the

ISBN 978-2-921145-88-6

solution process consists of using ray tracing to evaluate whether a given point in the computational domain is in direct sunlight or in shade for every timestamp present in the meteorological file provided. The ray tracing procedure is illustrated in Figure 1.

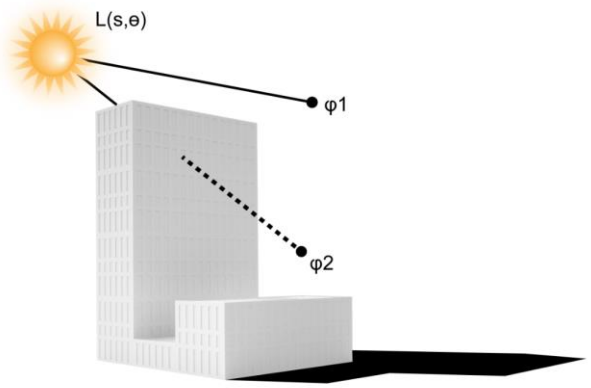

Figure 1: Ray tracing methodology used in the solar simulations.

Given a date and time, the elevation and azimuth of the sun relative to the site are computed; virtual "rays" are then projected from the sun point to every point in the test domain. If the ray is blocked by a building, then the associated path can be considered shaded from the sun. Diffuse exposure is computed using the model of Perez (1990) which was found to be suitable for cases where solar insolation is dominated by the direct contribution (as would be the case for any PV installation). During hours between sunset and sunrise, the entire domain is considered shaded and no solar loads are applied. The solver is executed in parallel, allowing for reduced simulation times. The shading condition for that timestep is combined with the solar radiation detailed in the weather file. These results are then combined into a variety of statistics including average and cumulative insolation

Solar Simulation Sensitivities

CAD Model Accuracy

The accuracy of the three-dimensional model used to represent the building being studied and its surrounds can have an impact on the quality of the results.

Figure 2 shows two CAD models of the same set of buildings. Of particular note is how the cylindrical building has been simplified. The low-detail model consists of an octagonal cylindrical shape while the detailed model retains a significant amount of surface detail including balconies and glazing. The podia have been similarly simplified. There are a variety of reasons why simplifying a complex geometry is beneficial including:

- Reduced model sizes help reduce simulation and rendering times and reduces storage requirements.
- In some cases, simpler shapes are used to create "water tight" geometries. This is particularly important if the solar simulations are to be coupled with computational fluid dynamics simulations
- Models are created for purposes other than simulation work, e.g. visualization only, hence simplified geometries are "fit for purpose".

To test the sensitivity of energy yield to CAD detail, we calculate the cumulative annual solar energy falling on the cylindrical building's surface for varying levels of refinement (in all cases, the balconies and glazing details were removed). Figure 3 shows the four cases analyzed, from the detailed model (icositehexagon – 26-sided polygonal section) to an octagonal cylinder. We also test the impact of rotating the octagonal cylinder by 22.5°, thereby eliminating the south-facing side of the polygon.

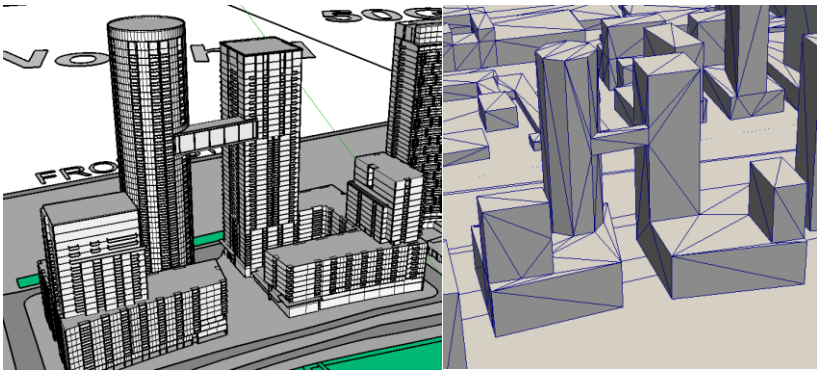

Figure 2: Two representations of the same set of buildings.
Left – detailed CAD model. Right – Simplified, low detail CAD model.

ISBN 978-2-921145-88-6

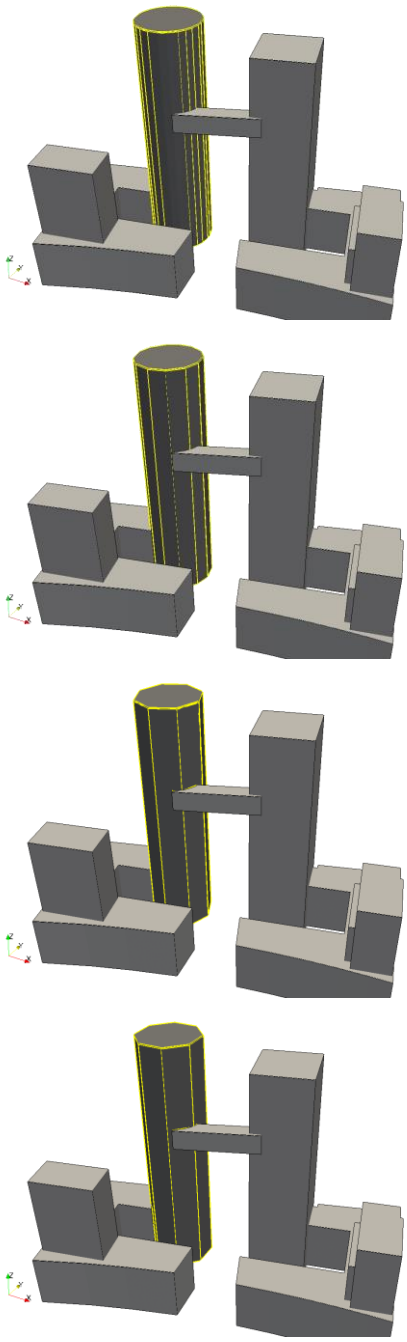

Figure 3: Top to bottom: detailed geometry (icositehexagon), tridecagon, octagon and rotated octagon

Table 1 shows the cumulative annual solar radiation for each of the configurations computed using a "typical" year of ambient weather conditions for Toronto (i.e. CWEC file for Pearson International Airport published by Environment Canada in EPW format). The cumulative solar radiation varied by less than 5% between even the most detailed (icositehexagon) and least detailed (octagon) models. Additionally, the rotated and unrotated octagons had similar total annual radiation levels although they did differ in terms of the locations of maximum insolation (not shown)

Table 1: Annual cumulative incident insolation on the building (absolute and relative to detailed model)

Configuration	Annual Cumulative Insolation [MWh]	Insolation Relative to Detailed [%]
Detailed	11,306	100.00
Tridecagon	11,191	98.98
Octagon	10,934	96.71
Octagon (Rotated)	10,934	96.70

Spatial Granularity

Simulating solar radiation impacting panels also requires a good understanding of how the computational cell sizes used to describe the panel impacts the overall results. Two questions arise:

- How does the energy estimate vary with computational cell size?
- Is prior knowledge of the orientation and configuration of the solar panel(s) important to accurately assess the energy production potential?

To test both questions, we examine a scenario where an existing building owner wishes to add either a flat or curved PV awning to a building located in the dense urban core of Boston, MA. The city model covers approximately 9 km² and is based on publicly available data which has been terrain corrected using high-resolution LiDAR survey data conducted by the National Oceanic and Atmospheric Administration (NOAA) (NOAA, 2017). The awning is approximately 12m long and extends 1.5m from the façade of the building, aligned horizontally. Figure 4 illustrates the awnings and a section of the surrounding domain.

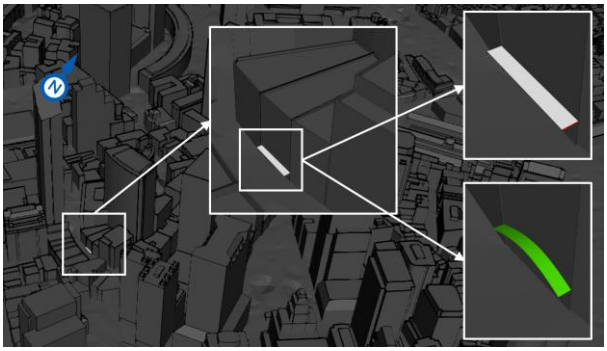

Figure 4: A portion of the surroundings urban context (grey) and the flat (white) and curved (green) PV awnings studied.

ISBN 978-2-921145-88-6

The awning surface was discretized into subsurfaces ranging in area from approximately 10m² to 0.01m² (i.e. dividing the awning in half, down to the scale of an individual solar cell). Each subsurface was tested for solar insolation at hourly increments using the standard TMY3 file for Boston. Table 2 summarizes the predicted annual cumulative insolation on the awnings for each simulation. For both designs, all simulations predict the same incident insolation to within 2%. Thus, for simple geometries spatial resolution appears to play a small role when estimating insolation falling upon a surface. Though, this will not always be the case. In the previous section, we showed that the accuracy of the underlying CAD model can influence energy predictions. This effect can be exacerbated if the spatial accuracy of the simulations is also low, as shown in Table 2 when comparing the curved panel results to the flat panel. In all cases, the curved panel experiences an incident energy penalty. However, the magnitude of the penalty changes depends on the spatial resolution. The coarsest resolution simulation predicts a loss more than four times larger than at the finest resolutions. A difference large enough to potentially change conclusions about the viability of the curved panel.

Table 2: Annual cumulative incident insolation for flat and curved panels

Subsurface Area [m²]	Annual Cumulative Insolation [kWh]		Curved % Loss Compared to Flat
	Flat	Curved	
9.5	17,394	16,927	2.7%
1.35	17,223	17,002	1.3%
0.46	17,176	16,882	1.7%
0.15	17,163	17,010	0.9%
0.041	17,121	17,006	0.7%
0.0085	17,113	17,011	0.6%

Inspecting Table 2 it is apparent that increasing spatial accuracy is best employed when attempting to understand differences in incident energy between different panel geometries. However, this only looks at the insolation falling on the panel itself, not the amount generated. Aside from the rated efficiency of the panel, how the individual solar cells are connected plays a large role in how much power is generated under a given condition. Each cell in a solar panel is connected in series into a "string" (see Figure 5). In many panels, shading even a single cell in a string can reduce the output of the whole string to zero. Technologies including bypass diodes and micro-inverters have been developed to minimize such impacts, however these technologies come with increased costs. The most inexpensive panels can have the entire panel on a single string.

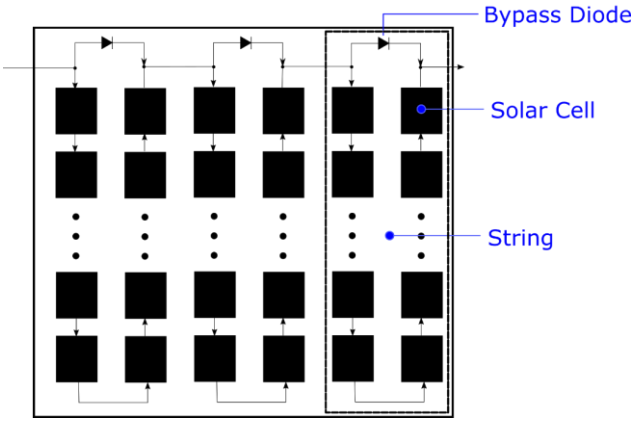

Figure 5: Solar panel composed of multiple strings of solar cells.

Predicting the effects of 'microshading' is critical to understanding the true potential of a BIPV site. Table 3 illustrates the results of a second analysis of the flat design, only with a conservative 'worst-case' panel model, where the entire panel is on a single string. In this type of analysis, the ability to simulate down to the individual solar cell becomes clear. The building to the west of the panel extends out approximately 0.15m and produces microshading effects that are not picked up at coarser resolutions. Having identified this potential, a designer can now re-evaluate the form and/or design of the panel to minimize the impact.

Table 3: Worst-case microshading loss on the flat awning

Subsurface Area [m²]	Microshading Loss (% of incident)
9.5	5.4%
1.35	5.2%
0.46	10.4%
0.15	15.4%
0.041	17.5%
0.0085	19.0%

To answer the questions asked at the beginning of this section; it is clear that for a fixed geometry the value of increasing spatial accuracy is minor when only attempting to compute incident energy potential. However, if there is a desire to better understand the actual production of energy, then increased spatial resolution is required to properly understand the effects of microshading and more complex geometries. Both of which are common in the realm of BIPV.

ISBN 978-2-921145-88-6

Temporal Granularity

Hourly simulations conducted over the course of a calendar year are the default approach for many forms of building performance simulation. However, the current level of computing power available to researchers and practitioners enables investigations at shorter timescales. Using the same cylindrical building simulation model described in the CAD model accuracy section, we now add four rooftop-mounted, inclined panels to assess the influence of the temporal fidelity of solar simulations in a BIPV context. The panels are resolved down to the scale of individual solar cells (0.01m²) and three simulations are conducted at 60, 15 and 1 minute timesteps. The panels are unshaded by neighbouring buildings but are shaded by a cellular telephone tower to the south of the panels (see Figure 6). Each panel is 10m long and 2m wide, inclined at 30°. The 15m high antenna is located approximately 11m to the south of the panels. The antenna's diameter is 60cm. We choose this simpler model as opposed to the more complex Boston model to better highlight the effects of temporal granularity. As the underlying Toronto CWEC data consists of hourly records, solar insolation at shorter timesteps is linearly interpolated to focus on the implications of the temporal accuracy of the simulations themselves. The ramifications of the temporal accuracy of the underlying climate data is discussed in the following section.

Figure 6 illustrates the simulation configuration and Table 4 shows the loss in annual cumulative insolation on each of the panels due to the antenna for each of the three timesteps.

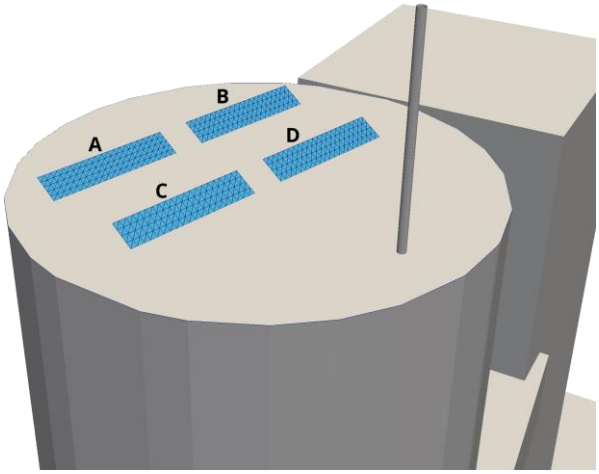

Figure 6: Test configuration. Four inclined panels with a cellular antenna directly to the south.

Table 4: Annual insolation lost due to antenna shadowing at various timesteps (absolute and relative to fully exposed condition)

Panel	60 minutes	15 minutes	1 minute
A	177 kWh (0.4%)	195 kWh (0.4%)	193 kWh (0.4%)
B	196 kWh (0.4%)	197 kWh (0.4%)	195 kWh (0.4%)
C	439 kWh (0.9%)	444 kWh (0.9%)	444 kWh (0.9%)
D	469 kWh (1.0%)	453 kWh (1.0%)	454 kWh (1.0%)
Total	1281 kWh (0.7%)	1289 kWh (0.7%)	1286 kWh (0.7%)

In terms of the overall loss in incident energy, reducing the timestep does not result in significantly different findings in this case. However, there is a subtler effect which emerges when examining which areas of the panels are being shadowed and what the local losses are.

Figure 7 is a plan view illustrating the local loss in insolation due to the antenna across each panel for each of the studied temporal resolutions. While the aggregated losses are similar between each of the simulations, the locations where the losses occur and their magnitudes vary much more significantly. For example, the southeast corner of Panel C was predicted to lose approximately 80 kWh/m² by the 60 minute simulation, whereas the 15 and 1 minute simulations predict a loss of less than 40 kWh/m². Conversely, an area 0.6m to the west of that corner is predicted to have a similar 40 kWh/m² insolation loss under the 1 and 15 minute simulations, which the 60 minute simulation misses entirely. Thus, in this simple example, the value of the smaller timestep lies not in the estimation of overall insolation, but rather the ability to accurately resolve microshading effects across the panel. As noted above, capturing these effects allows for improved siting of panels and potentially even optimizing the configuration of the strings and cells to minimize partial shading losses based on small scale microshading effect common in BIPV applications.

If the simulations are repeated using the previously described PV cell string model to account for micro-shadowing, we find that the resulting energy losses can be significantly reduced through thoughtful string configuration (summarized in Table 5). Understanding the trade-off between energy yield and panel complexity (and thus cost) is a key consideration particularly when integrating PV into complex facades.

ISBN 978-2-921145-88-6

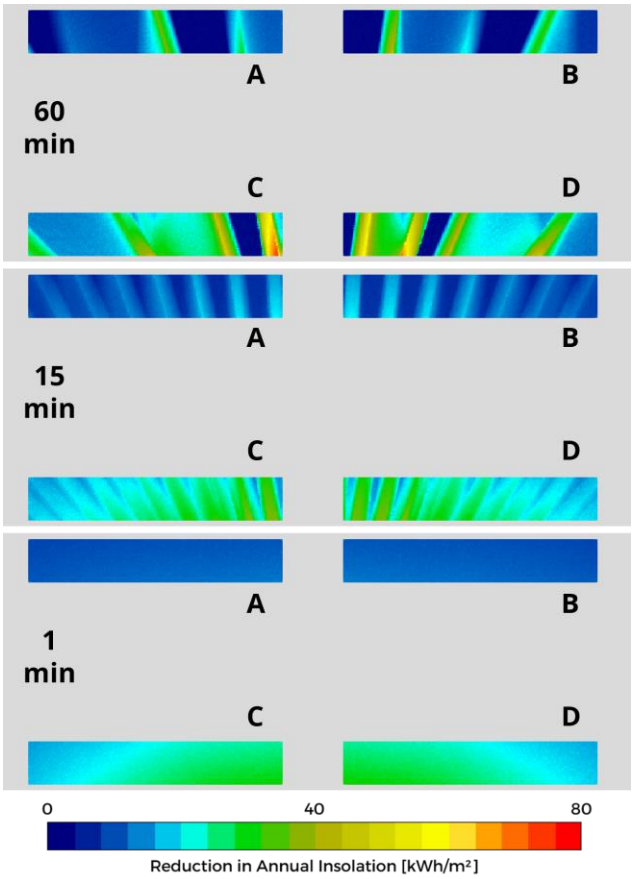

Figure 7: Insolation loss contours simulated at three temporal resolutions

Table 5: Percentage loss in total annual energy under various string configurations

String Configuration	Energy Loss [% of Unshaded]
1 string per panel	11%
2 strings per panel (horizontal)	10%
2 strings per panel (vertical)	6%
10 strings per panel (vertical)	2%
100 strings per panel (vertical)	1%

Weather Data

Typical Meteorological Year (TMY) files are ubiquitous within the building performance simulation community, providing the ambient meteorological parameters critical to many forms of building simulation. However, aside from selecting the closest station to the site, little thought is often given to the appropriateness of the data set for the given task. At first glance using TMY files for solar energy investigations may seem appropriate since the weighting algorithm used to define the "typicality" of a given month is heavily weighted towards solar radiation (Wilcox, 2008). However, one must be careful when using these files, as the assumptions and limitations that go into them can bias results in subtle, but potentially important ways.

Temporal Resolution of Input Data

The TMY/EPW format consists of 8760 hourly records providing a "typical" year's worth of meteorological data. As described in the previous section, temporal accuracy can influence results through the exaggeration of shading impacts in some areas, and missing them entirely in others which is a key drawback of these files in a BIPV context.

Increasingly, simulation practitioners can access solar data at sub-hourly time-scales through both no-cost resources (e.g. the National Solar Radiation Database (NSRDB) published by NREL (Sengupta, 2015)) and for-profit services. This ease of access, coupled with the ever-increasing accessibility of large scale computing resources, means that it is easier than ever to employ these refined datasets.

Typicality of Other Parameters

The typical year algorithm is based on monthly and annual statistics, meaning that variations and trends at shorter timescales cannot (and should not) be assumed to be typical. Cloud cover is highly dynamic and while there are typical monthly and annual averaged amounts of cloud cover, a typical level of cloud cover at a specific time on a specific day does not exist. The lowered solar irradiance at such times can potentially act to mask the effects of shadowing because of the lowered hourly insolation level.

To illustrate these considerations, annual solar insolation on a large greenspace within a complex urban core (Boston Common in Boston, USA) is simulated using two sources of weather data: the TMY3 file for Logan International Airport and 18 years of solar data, taken at 30 minute increments at the site sourced from the NSRDB. The intention of this example is to mimic a solar siting study within a dense city on a complex surface. As such the landscaping in the Common has been intentionally ignored. Figure 8 below illustrates the test surface of Boston Common and a portion of the surrounding built environment.

ISBN 978-2-921145-88-6

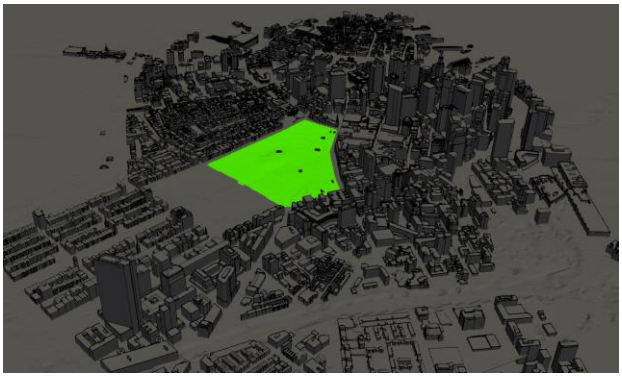

Figure 8: 3D model of Boston Common (green) and surrounding urban context (grey).

Figure 9 presents contour plots of the predicted annual insolation across the Common using the NSRDB solar data and TMY3 solar data as inputs, as well as difference between the two data sets, expressed as a percentage difference from the NSRDB based results. The TMY3 based data resulted in uniformly lower insolation predictions, ranging in magnitude from 4% to 9%, resulting in a mean underprediction across the entire area of approximately 6%. In other forms of simulation underpredictions of this magnitude are often inconsequential, however for BIPV systems a 9% difference in yield could be the difference for a system's economic viability. Additionally, the significant spatial variability of the underprediction could lead to a larger problem of less-than-optimal positioning of PV systems.

Figure 10 illustrates similar plots showing the reduction in insolation caused by the addition of a new tall building to the southeast. The discrepancies between the NSRDB and TMY3 based results are now larger. The TMY3 based results indicate a smaller area of the Common affected by the building, but the area that is affected is impacted to a much greater degree. The TMY3 based results predict insolation losses in some areas which are more than twice the losses predicted using the NSRDB data. More disturbing is the fact that not only are there very large overpredictions of insolation loss, but also equally large underpredictions of the building's impact. In one area of the Common, the TMY3 based data transitions from a 50% overprediction to a 50% underprediction within 20m. It is the hourly timestep of the TMY3 data which results in the "concentration" of the energy loss, assigning an entire hour's energy loss within a single area, rather than smearing the loss over a larger area as the building's shadow moves over the course of that hour. The areas where the TMY3 based data fails to identify shadow impacts are likely caused through a combination of some smaller scale showing being missed because it occurs between the hourly steps and cloud cover. Figure 11 compares average solar insolation statistics between the two sources of solar data during the range of solar positions where the new building can cause shadow. Average insolation is dramatically lower during the shoulder seasons, even during February, August and October, which based on the NSRDB data, is when the sky in Boston is significantly clearer. This lower average insolation can mask the effects of shadowing and skew overall solar potential in a spatially inconsistent fashion.

If a practitioner were attempting to understand the effects of the proposed building on existing or future PV systems based on the TMY3 based results. It would be possible for them to overstate the impact in some areas while simultaneously understating the impact in others. This could lead to unnecessary or ineffective changes to a proposed building, the relocation of existing PV to non-ideal locations or even the cancellation of a PV system outright.

While this study focuses on PV siting in a more traditional context (i.e. ground-mounted), BIPV is potentially more sensitive to these impacts since accurate siting of BIPV systems to avoid shading and minimize the payback period is critical to them surviving the value engineering phase of modern building design.

ISBN 978-2-921145-88-6

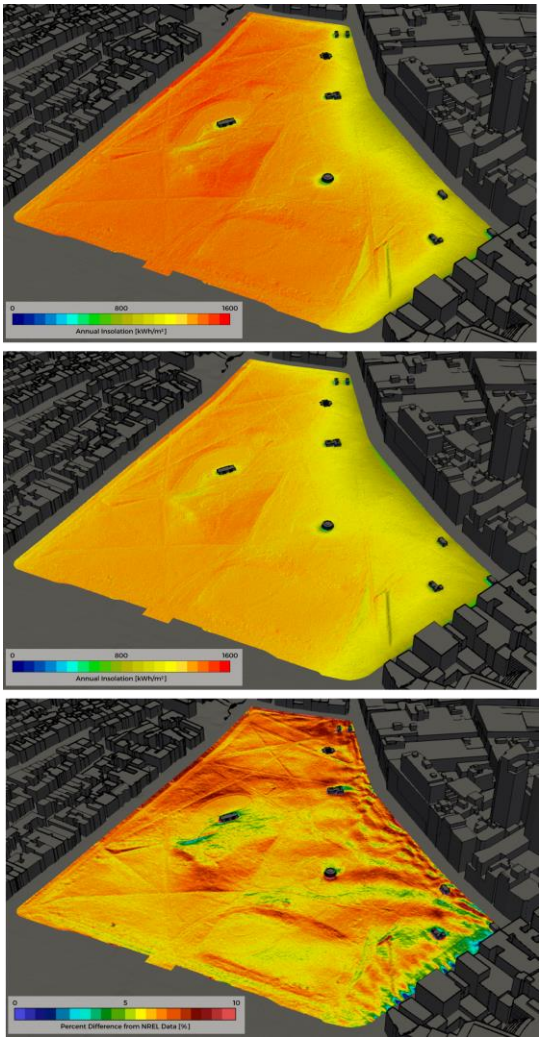

Figure 9: Contour plots of annual insolation based on NSRDB data (top) and TMY3 data (centre), as well as the resulting difference between the two predictions (bottom).

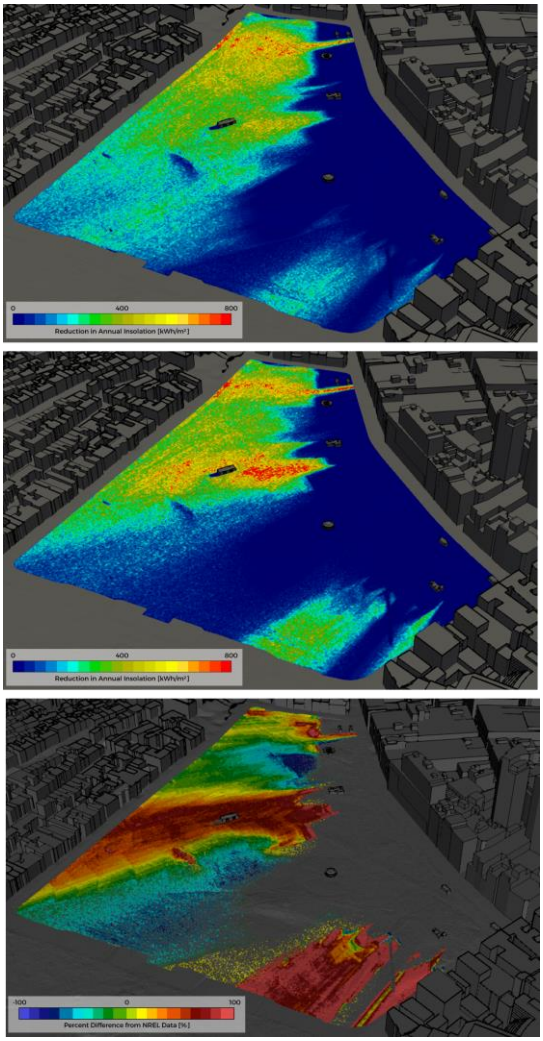

Figure 10: Contour plots of insolation lost due to a proposed building based on NSRDB data (top) and TMY3 data (centre), as well as the resulting difference between the two predictions (bottom). Areas unaffected by the building are excluded in the bottom image for clarity.

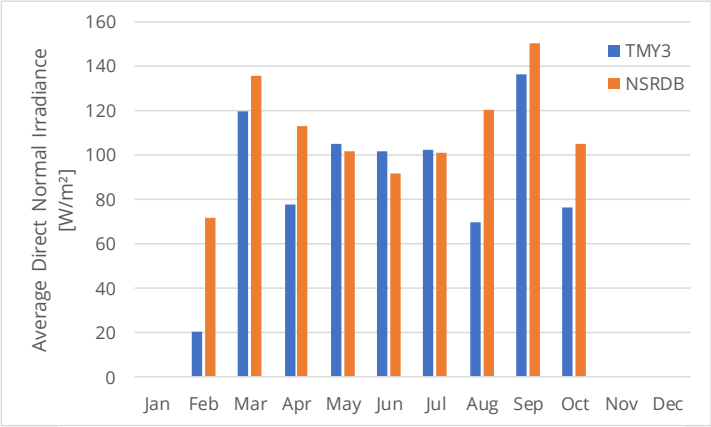

Figure 11: Comparison of monthly average solar insolation during shadow events.

ISBN 978-2-921145-88-6

BIPV AND THE URBAN ENVIRONMENT

There are a variety of challenges associated with integrating BIPV into the urban environment. Understanding how BIPV interacts with the local climate (microclimate) is particularly important. Minimizing negative impacts on the building, surrounding structures, pedestrians and residents should be prioritized when designing BIPV systems. To this end, there are a variety of simulation and testing procedures that can (and should) be used to identify potential design flaws and quantify impact on the building and its surroundings.

Wind Effects

As with any exterior building element, solar panels must withstand the wind conditions within which they are placed. Rooftop installations, e.g. on the roof of a tall, isolated tower, require a detailed understanding of the local wind climate. Winds around buildings are often turbulent and gusty, creating high pressure loads on the panels which can lead to structural failure and safety issues. Placing solar panels on a rooftop or even integrating them into a building can also alter the wind behavior around a building. For example, rooftop panels will alter how the rooftop recirculation zone is formed, thereby altering the expected wind speeds on the roof and potentially influencing intake and exhaust systems.

Computational fluid dynamics (CFD) modelling or wind tunnel testing can help quantify such impacts. Though computing accurate wind pressure information with CFD is not a trivial undertaking (Tamura 2008) and if not done correctly can lead to incorrect results and significant safety risks.

Snow and Ice

Roof mounted PV panels have a significant impact on the snow/ice accumulation characteristics of a roof or facade. This is particularly evident on large warehouse rooftops which provide large surface areas. This can have an impact on the structural integrity of the roof itself or create potentially dangerous instances of sliding ice and snow falling onto occupied areas.

One can test the impact of the rooftop installation on snow loading and deposition using a water flume (Brooks, 2015) or computationally (Tominaga, 2011). Figure 12 shows an example of a flume study. Sand particles are injected into an immersed channel with a physical model of the building. The relative density of sand to water is equivalent to that of snow to air. The deposition patterns provide a qualitative understanding of the expected snow loads. This can also provide an understanding of snowfall related production losses which can occur.

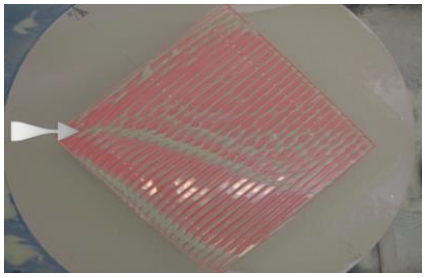

Figure 12: Flume testing showing expected snow deposition patterns on a large rooftop PV installation.

Glare

BIPV can also change the amount of glare from a building. Glare refers to unwanted solar reflections from a surface. These reflections can impact neighboring buildings, pedestrians and drivers. The impact of glare ranges from being an annoyance to affecting the ability of drivers, pilots and air traffic controllers to see (Jakubiec, 2014). Assessing glare potential is an increasingly common requirement during building design. The primary challenge predicting glare from BIPV systems lies in the fact that their reflectance characteristics are often not well documented by manufacturers. Care must be taken to ensure material properties are well understood and implemented appropriately in glare simulations.

Figure 13 shows an example of the source of a glare event being forensically determined through simulation. The photo on the right was taken on site and the lines in the image on the left identify sun ray paths to the source.

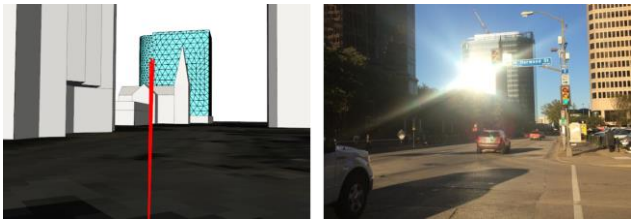

Figure 13: Computational simulation of a glare event

Heat Gain

PV panels are also prone to significant heat gains. Solar radiation absorbed by the panel is either converted into electric energy or heat. Since conversion efficiency tend to be quite low, this can result in a significant amount of the radiation being converted to thermal energy. Panel temperatures can be significantly higher than ambient. Under sunny, warm conditions, panels can reach over 80°C. Not only do these panels pose a danger to anyone standing close to them, but heat released from the panels can be entrained into nearby buildings (or impact building intake locations). CFD can be used to determine the impact that an increase in panel temperature has on its

ISBN 978-2-921145-88-6

surroundings. Figure 14 shows PV panels mounted approximately 2m above a rooftop. The panels heat up in the sun and convectively reject heat (along with other mechanisms). This heat is transported downwind, potentially impacting occupied areas or building intakes.

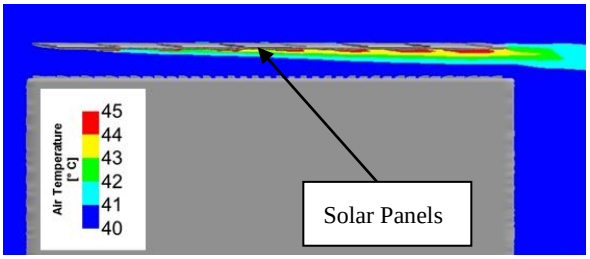

Figure 14: Increase in air temperature due to solar panel heating

CONCLUSIONS

BIPV is a tremendous opportunity to make the built environment more resilient and sustainable. However wide-spread deployment can be challenged by perceptions that such systems are not economically viable or that they come with other risks. Early simulation can be used to allay such concerns, but practitioners must ensure that the methods developed for simpler situations are still appropriate for a scenario as complex as BIPV in the urban realm.

For basic analyses of annual average insolation falling on simple surfaces, industry standard practices for geometric simplifications and temporal accuracy were found to provide reasonable results. However, as surfaces become more complex or if more refined predictions of energy generation are required, the standard approaches resulted in problematic levels of error. Discretizing test surfaces to the scale of individual solar cells and simulating shadow effects at time scales well under an hour, provided significant insights into optimal design of PV systems in complex environments. Climate data proved to be a critical source of error for even relatively simple surfaces when the analysis went beyond a simple estimation of average annual insolation. Thus, employing longer term solar insolation records which have been recorded at sub-hourly time steps should be employed as often as practical.

Solar and fluid simulations can also be used to evaluate the impact of PV and BIPV installations on the local environment. Glare, heat island, snow and wind loading are some of the potential issues that should be understood and addressed early in the design process to prevent post-construction impacts on people and property. Though care must be taken that these studies are conducted by those with sufficient expertise to properly understand and predict these impacts.

The practices suggested in this text are by no means definitive; however, we do hope that this spurs further discussion between governments and the academic and industrial communities and helps move towards the creation of robust and effective guidance for the safe and efficient integration of photovoltaics into the urban fabric.

ACKNOWLEDGEMENTS

The authors thank those who provided insightful comments and suggestions on this text and acknowledge the support of our employer during the development and publication of this work.

REFERENCES

Brooks, A., et al, 2015. Rapid Assessment of Snow Drifting Conditions Using Physical Model Simulations. *Cold Regions Engineering* 2015 (pp. 310-321).

Chiabrando, R., et al, 2009. The territorial and landscape impacts of photovoltaic systems: Definition of impacts and assessment of the glare risk. *Renewable and Sustainable Energy Reviews*, 13(9), pp.2441-2451.

Danks, R., 2014. Applications of Large Scale Solar Modeling in the Built Environment. In *Proceedings of the eSim 2014 Building Performance Simulation Conference of IBPSA-Canada*, May 8-9, pp. 562–574. Ottawa, ON.

Dobos, A.P., 2014. PVWatts version 5 manual (No. NREL/TP-6A20-62641). National Renewable Energy Laboratory (NREL), Golden, CO.

RetScreen. (2005). Varennes, QC: Natural Resources Canada.

Jakubiec, J. and Reinhart, C., 2014. Assessing disability glare potential of reflections from new construction: Case study analysis and recommendations for the future. *Transportation Research Record: Journal of the Transportation Research Board*, (2449), pp.114-122.

NOAA. 2017. Office for Coastal Management. Coastal Topographic Lidar. Last Accessed December 2017. <https://www.coast.noaa.gov/dataviewer/>

Perez, R., et al, 1990, Modeling Daylight Availability and Irradiance Components from Direct and Global Irradiance, *Solar Energy*, 44(5), pp. 271-289

Sengupta, M., et al, 2015. Validation of the National Solar Radiation Database (NSRDB) (2005-2012).

Tamura, T., et al, 2008. AIJ guide for numerical prediction of wind loads on buildings. *Journal of Wind Engineering and Industrial Aerodynamics*, 96(10-11), pp.1974-1984.

Tominaga, Y., et al, 2011. CFD modeling of snowdrift around a building: An overview of models and evaluation of a new approach. *Building and Environment*,46(4), pp.899-910.

Wilcox, S. and Marion, W., 2008. Users manual for TMY3 data sets (pp. 4-5). Golden, CO: National Renewable Energy Laboratory.

ISBN 978-2-921145-88-6